Chapter 9

Graphene Nanocomposites Studied by Raman Spectroscopy

Elena Iuliana Bîru and Horia Iovu

Additional information is available at the end of the chapter

http://dx.doi.org/10.5772/intechopen.73487

Abstract

The goal of this chapter is to provide a general introduction about graphene nanocomposites studied by Raman spectroscopy. The chapter will therefore begin with a brief description of the major Raman bands of carbon allotropes. In the following chapter a concise comparison between single walled carbon nanotubes (SWCNTs), multi-walled carbon nanotubes (MWCNTs), fullerenes and graphene is exposed. The characteristic features in Raman spectra of carbon allotropes, namely the intense signals D and G are investigated. In particular, the chapter will outline the Raman spectrum of graphene and different types of graphene oxide. The last part of the chapter is devoted to graphene nanocomposites.

Keywords: carbon allotropes, carbon nanotubes, graphene Raman bands, graphene oxide, polymeric nanocomposites

1. Introduction

As a nondestructive chemical analysis technique, Raman spectroscopy has become a powerful research tool providing detailed information about chemical structure and identity, phase and polymorphism, molecular interactions and crystallinity. Raman spectrum is a distinct chemical fingerprint for a particular molecule or material and it can be used to quickly identify the sample, or distinguish it from others. Therefore, Raman spectroscopy may be used in any application where nondestructive, microscopic chemical analysis or imaging is required. The use of Raman spectroscopy initially originating in physics and chemistry analysis has now spread to a variety of applications in materials science [1] or even in biology for ultrafast reveling of bacteria [2] and medicine [3].

Recently, carbon materials have revolutionized the field of material science. In order to illustrate the importance of Raman spectroscopy in the field of carbon nanocomposites a short description of some representative carbon allotropes will be exposed. Due to its unique electronic structure, carbon is an element available in a variety of structural forms being able to form sp^3, sp^2 and sp hybridization networks more stable than any other element. Carbon nanomaterials offer a wide range of useful properties such as large specific area [4], excellent electrical conductivity [5], high Young's modulus [6] and thermal conductivity [7]. Raman spectroscopy is an important tool for the characterization of carbon nanomaterials offering valuable information about the existence of structure defects or further functionalization.

Although carbon materials are all entirely made of C-C bonds, the orientation of these bonds is different for each type of carbon allotrope. All these materials are exclusively composed of pure carbon but are different structural forms and exhibit quite different physical properties and chemical behavior. Carbon exists in two allotropic forms: crystalline allotropes (diamond, graphite, fullerene, carbon nanotubes) and amorphous allotropes (carbon black, coke, charcoal).

Diamond is the hardest material on earth and finds applications in cutting, drilling, and jewelry. In diamond structure each carbon atom undergoes sp^3 hybridization and it is linked with four other carbon atoms in a tetrahedral structure. Diamond does not conduct electricity because it does not exhibit any delocalized electrons.

Graphite has a layered structure and all these layers are held by Van der Waals forces. In graphite structure each carbon atoms is sp^2 hybridized and each layer is composed of hexagonal rings of carbon atoms.

Fullerenes are made by heating graphite in an electric arc in the presence of inert gas. These carbon allotropes are cage like structures, with all carbon atoms sp^2 hybridized.

Carbon nanotubes (CNTs) exhibit the form of cylindrical carbon molecules and exhibit unique features that make them extremely useful in a plethora of applications especially in nanotechnology, electronics, optics and many other fields of materials science. A carbon nanotube can be defined as a tube-shaped material, entirely made from carbon, having the diameter measuring on the nanometer scale. A carbon nanotube can be as thin as a few nanometers but as long as hundreds of microns [8]. CNTs are at least 100 times stronger than steel, but only one sixth as heavy, so nanotube fibers could strengthen almost any material [9]. Nanotubes may conduct heat and electricity better than copper. CNT are already incorporated in polymer composites to control or enhance conductivity. Carbon nanotubes may be classified as single-wall (SWCNTs) or multi-wall nanotubes (MWCNTs). SWCNTs can be simply envisaged like a regular tube entirely made of carbon atoms. In contrast to single-wall carbon nanotubes, the MWCNTs are an assemblage of an outer and at least one inner carbon tube separated one from another by interatomic forces.

Graphene is a thin single layer of pure carbon. Graphene was firstly isolated in 2004 by two researchers from The University of Manchester using the "scotch-tape" technique [10]. Basically graphene consists in a monolayer of graphite. In more complex terms, graphene is a two dimension honeycomb single layer crystal lattice formed by the tightly packed sp^2 bonded

http://dx.doi.org/10.5772/intechopen.73487

carbon atoms [11]. Having excellent thermal, mechanical, electrical and barrier properties [12], graphene is recommended for many applications such as: electronics [13], antimicrobial materials [14], construction materials [15], battery [16] and supercapacitors etc. More details about graphene and other graphene derivatives will be exposed in section 2 of this chapter.

In order to differentiate these materials there is a strong demand for techniques that can be used to characterize them. As a remarkably sensitive technique, Raman spectroscopy suits perfectly on these demands, being highly responsive to symmetric covalent bonds with very little or no dipole moment. Raman spectroscopy is capable of discerning any slight changes in structure.

When monochromatic radiation is incident upon a carbon allotrope sample the light will interact with the sample in a specific way. Every bond in the Raman spectrum corresponds directly to a specific molecular bond vibration, including bonds such as C-C, C=C, C-H etc. As a chemical fingerprint of the material, the general spectrum profile (peak position and intensity) provides unique information which can be used to identify the material and distinguish it from others.

When comparing the Raman spectra of two carbon allotropes – diamond and graphite – significant differences between these two materials can be noticed even if both are entirely made of C-C bonds (**Figure 1**). The Raman spectrum of pure diamond exhibits an extremely sharp signal at ~1332 cm^{-1}. The Raman spectrum of graphite shows different features compared to diamond. Two distinguishable peaks are revealed at ~1350 cm^{-1} (D band) and ~1580 cm^{-1} (G band). The G band arises from the stretching of the C-C bond in graphitic materials and it is common to all sp^2 carbon systems. The presence of an additional band in the graphite spectrum reveals that graphite is not as uniform in structure as diamond. The D-mode in graphite is induced by disorder or defects and increases linearly with decreasing graphite crystallite size (**Figure 2**).

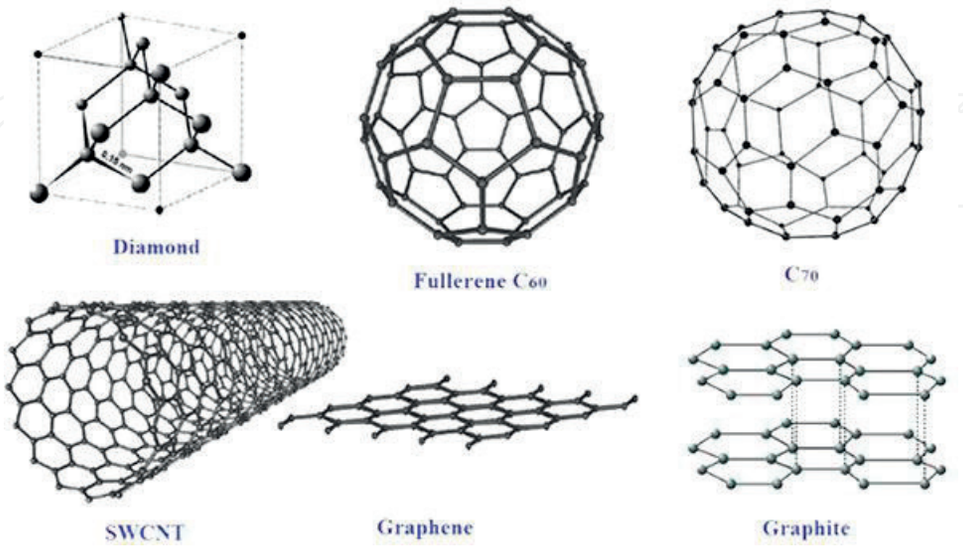

Figure 1. Structure of the most representative carbon allotropes.

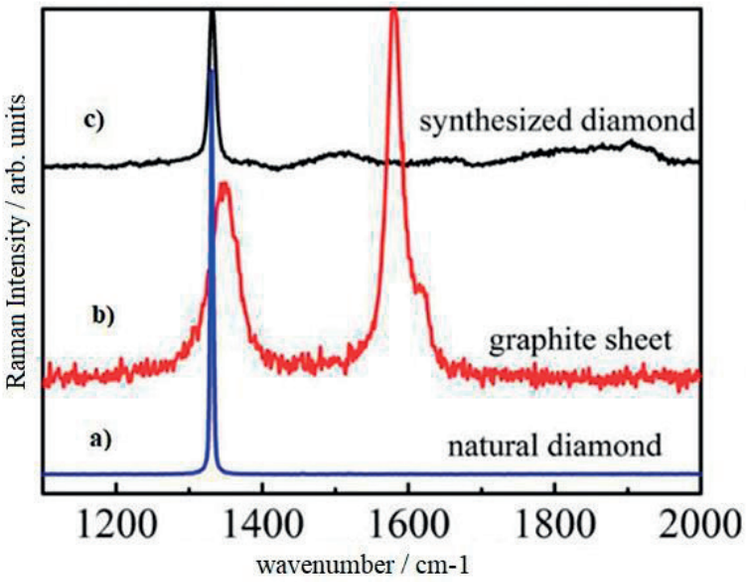

Figure 2. The Raman spectra for a) natural diamond and c) synthesized diamond compared with b) Raman spectrum of graphite (Yao K et al. (2017) copyrights) [17].

More complex structures can be also investigated by Raman spectroscopy. Fullerenes have attracted much attention for their applications in non-linear optics [18] or biomedical devices [19]. C60 (also called Buckminster fullerene) and C70 have been investigated in a large number of experiments because of their potential applications fabrication of nanodevices such as field effect transistors and flat panel display devices based on field emission [20].

Figure 3 compares the Raman spectra of C60 and C70. The Raman spectrum of C60 exhibited strong signals at 1467 cm^{-1} and 1567 cm^{-1}. This fact reveals that C60 is composed of sp^2 bonded carbon and the sharpness of the signal shows that C60 exhibits a uniform structure. On the contrary, the Raman spectrum of C70 exhibits numerous other peaks. In case of C70 film, the main peaks are located at 1564 and 1228 cm^{-1} due to a reduction in molecular symmetry which results in more Raman bands. Their relative intensities strongly depend on the excitation laser wavelength.

Until 1980 only four carbon allotropes were known: graphite, amorphous carbon, fullerenes and diamond. Since their discovery in 1991 by Dr. Sumio Ijima, carbon nanotubes (CNTs) have gained tremendous attention as a versatile nanomaterial with abundant applications. Like previously mentioned, CNTs are carbon allotropes with a cylindrical nanostructure.

CNTs are essentially rolled up graphene sheets that have been sealed to form hollow tubes (**Figure 1**). Depending on the number of concentrically rolled-up graphene sheets, CNTs are classified to single-walled (SWCNT), double-walled (DWCNT), and multi-walled CNTs (MWCNT). The structure of SWNT can be imagined by wrapping a one-atom-thick layer of graphene into a seamless cylinder. DWCNT is considered as a special type of MWCNT wherein only two rolled up graphene sheets are present. MWCNT consists of two or more numbers of rolled-up concentric graphene sheets [22]. The diameter of SWCNT is generally up to 2 nm. In case of MWCNTs the diameter varies from 5 to 20 nm, seldom exceeding 100 nm [23].

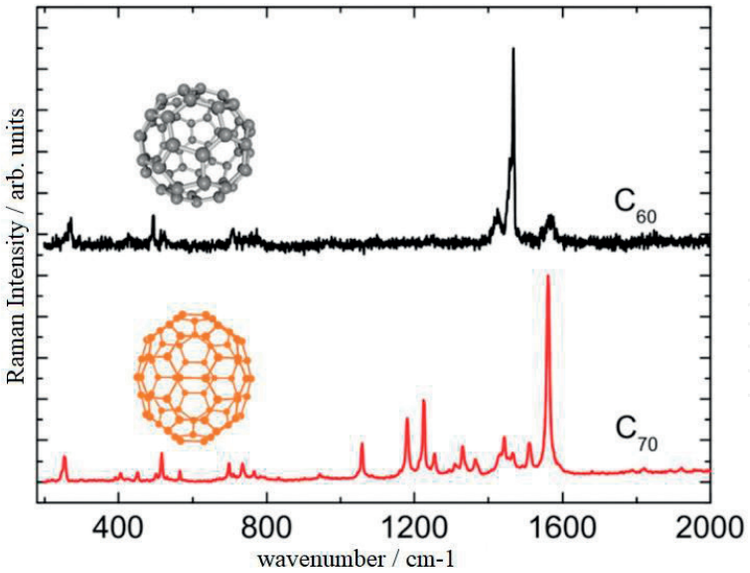

Figure 3. Raman spectra for C60 and C70 films. The insets show the molecular structures for C60 and C70 (Zhang X et al. (2016) copyrights) [21].

Having remarkable properties such as high electrical conductivity, very high tensile strength and low thermal expansion coefficient, CNTs have been investigated for many applications such as composite materials, microelectronics and electronic components, solar cells, energy storage devices [24] etc. In addition, their one-dimensional structure makes them an ideal platform for biomedical applications. Due to their important applications a significant number of methods to produce CNTs were developed: arc discharge method [25], laser method [26], chemical vapor deposition (CVD) [27], ball milling [28], etc. Final properties of CNTs are dependent on the production and purification methods.

In **Figure 4** a comparison of Raman spectra of graphite, SWCNTS and MWCNTs is depicted. The stretching of the C-C bond in graphitic materials gives rise to the so-called G-band Raman feature which is common to all sp^2 carbon systems. This spectral feature is similar for graphite and nanotubes but is not used for distinguishing one carbon nanostructure from another. The G-band is highly sensitive to strain effects in sp^2 carbon materials and can be used to investigate any modification to the structure of graphene, such as the strain induced by external forces in multiwall nanotubes, or even by the curvature of the side wall when growing a SWCNT [29]. A prominent G band can be noticed in the graphite Raman spectrum at ~1580 cm^{-1}. As one can see the G band is present also in the SWCNT and MWCNT spectra but with different width. The G-band of investigated SWCNTs splits in two band components because of large diameter nanotubes and it can be used to distinguish metallic and semiconducting nanotubes.

Another important band in the Raman spectra of the investigated nanotubes at ~1350 cm^{-1} was observed known as the D band. The D band is caused by disordered structure of graphene sheets. The presence of disorder in sp^2-hybridized carbon systems results in resonance Raman spectra as one can see in the Raman spectrum of CNTs making Raman spectroscopy one of the most sensitive techniques to characterize disorder in sp^2 carbon materials. In case of CNTs the D band is significantly increased compared to graphite. The increase of the ratio

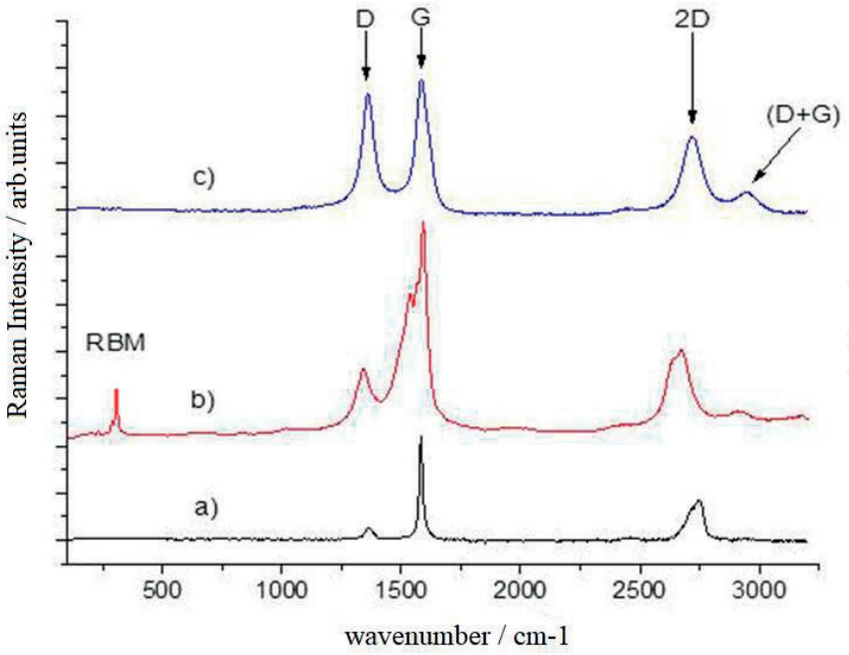

Figure 4. The Raman spectra of a) graphite, b) single wall carbon nanotubes (SWCNTs) and c) multiwall carbon nanotubes (MWCNTs).

between the intensity of D band and the intensity of G band (I_D/I_C) indicates that some disorder of the graphene sheets is induced. As previously mentioned graphite consists of stacks of planar sheets of graphene and carbon nanotubes are basically rolled-up graphene sheets. Therefore the presence of the 2D band (also named G` band) is observed in all spectra of the investigated samples which features the arrangement and the number of graphene layers [30]. The importance of the 2D band of graphene will be better explained in section 2 of this chapter. The radial breathing mode (RBM) is particularly important for the determination of the diameter of CNT, its frequency being related to the aggregation state of SWCNTs. The RBM band is unique to SWNCTs and corresponds to the expansion and contraction of the nanotubes. Comparing the Raman spectrum of MWCNTs to that of SWCNTs some important differences can be easily noticed: the absence of RBM mode in MWCNTs spectrum and much sharper D peak in MWNCTs. The RBM band is not present in case of MWNCTs due to the outer tubes that restrict the breathing mode. The presence of a more outlined D band in case of MWCNTs is observed because of the multilayer configuration of nanotubes suggesting a more disordered structure. In addition, a sharper D+G combination peak strongly supports the presence of higher disorder in the MWCNTs, compared to SWCNTs.

2. Graphene and graphene oxide

Even if for several decades the isolation of single layer graphite seemed to be impossible two researchers from Manchester University successfully managed in 2004 to isolate monolayer graphite. The "scotch-tape" technique reported by Geim and Novoselov consisted in obtaining

single layer of graphene on a silicon oxide substrate by peeling the graphite by micromechanical cleavage [10]. In 2010 the two researchers won the Nobel Prize in Physics for their pioneering study [31]. Several methods have been established for graphene production, such as micromechanical or chemical exfoliation of graphite [32], graphitization of silicon carbide [33], chemical vapor deposition (CVD) growth [34], and chemical, thermal or electrochemical reduction of graphene oxide [35].

Graphene is a one-atom-thick planar sheet of sp2-bonded carbon atoms that are densely packed in a honeycomb crystal lattice [36]. Due to its 2D nature graphene exhibit a unique combination of characteristics not seen in other carbon allotropes. Graphene is the thinnest, strongest and stiffest material [37]. Graphene has extraordinary electrical properties due to the high electron mobility at room temperature [38]. In terms of mechanical properties graphene exhibit greater performances when single or few layer graphene are employed. Therefore, the superior mechanical properties of graphene and its derivatives make them the ideal candidates for incorporation into a large variety of materials in order to produce composites with enhanced properties.

Graphene also exhibits other high characteristics such as large specific surface are, high transparency and high thermal conductivity. Because of its high surface area graphene also finds potential applications as support material in catalysis field as an electrode material in electrochemical applications such as supercapacitors and batteries [39].

Due to these extraordinary properties, graphene found already a great number of important applications with potential used in touch screens displays, fuel cells, intelligent coatings, transparent conductive films and flexible electronics [40]. In addition, once functionalized with biomolecules like polysaccharides [41], proteins [42], etc. or other biological systems graphene can be integrated for developing new applications in biomedicine and bio-nanotechnology such as biosensors [43], biocatalysis [44], biofuel cells [45], etc.

It is worth noting that the electronic properties of graphene drastically depend on the number of graphene layers. For that reason, the graphene community distinguishes between monolayer graphene, bilayer or few-layer graphene. A structure composed of more than 10 graphene layers exhibits the electronic properties of graphite and therefore is considered as a thin film of graphite. Being transparent as well as a good conductor, graphene may replace the electrodes in the indium used in touchscreens [46].

In order to integrate graphene into various functional structures or other materials for making performant nanodevices one preliminary condition is required: graphene sheets have to be exfoliated into individual or few-layer sheets and stabilized. Also, unwanted by-products and structural damage can be produced while synthesizing graphene. A quick and precise method for determining the number of layers of graphene sheets is essential for speeding up the research and exploration of graphene. In sp2-bonded carbon species, as a highly sensitive and non-destructive technique, Raman spectroscopy can be used to investigate the number of layers, the type and relative quantity of defects, mechanical strain, and any further functionalization. Therefore Raman spectroscopy is one of the most powerful tools available for analysing graphene.

In specific case of graphene, Raman spectroscopy can evaluate not only the number of graphene layers, but also can provide a quick and non-destructive means to distinguish monolayer, bilayer and few layer graphene. The most prominent Raman features of graphene are the so-called G band and 2D as easily seen in **Figure 5**, which depicts a typical Raman spectrum for graphite and graphene respectively obtained using a 514 nm excitation laser.

Graphite consists of sp^2 bonded planar graphene sheets stacked through Van der Waals intermolecular forces. When comparing the Raman spectra of graphite and graphene one can observe a tremendous similarity. The reason for that is the fact that graphite consists in multiple stacked graphene layers. As in the case of graphite, the G mode from graphene occurs around 1580 cm^{-1} and the 2D signal is situated around 2700 cm^{-1}. Two further signals can be noticed: the D band that is observed at ~1350 cm^{-1} and 2D` band at ~3250 cm^{-1}.

In terms of vibrational behavior, the G band originates from in-plane stretching vibrations of sp^2 carbon atoms in both rings and chains. Even at low intensity the D mode can be observed in the Raman spectrum of graphene which occurs due to the breathing modes of sp^2 carbon atoms rings. Generally the D mode is associated with the presence of graphene structural defects. When the D band is higher it means that the sp^2 bonds are broken and new sp^3 bonds are created. Consequently the increase of the ratio between the intensity of D band and the intensity of G band (I_D/I_C) demonstrates that new defects are created during the modification of pristine graphene.

The D mode is almost absent in well-ordered structure of graphene and graphite. Despite the similarities, there are some significant differences as one can notice in **Figure 5**. In case of pure graphene the 2D band situated at ~2700 cm^{-1} is much sharper. The 2D band originates from a two-phonon double resonance process and it is interrelated to the band structure of graphene layers. **Figure 5(b)** indicates a significant change in the shape and intensity of the 2D band of graphene compared to graphite. It can be easily observed that in case of graphene the 2D peak is much narrower and its position is down-shifted. Another difference is observed in the

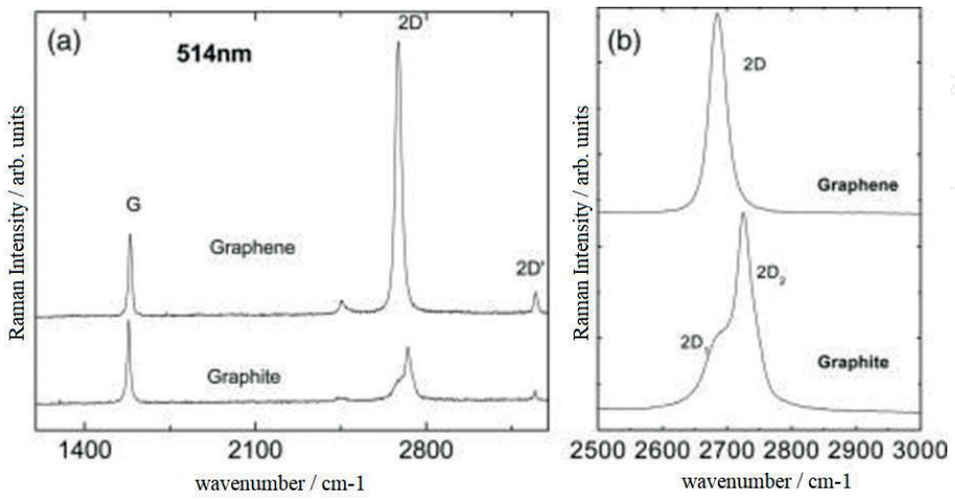

Figure 5. (a) The Raman spectra of graphene and graphite measured at 514.5 nm. (b) 2D peaks in graphene and graphite (Ferrari A (2007) copyrights).

Raman spectrum of graphite in which the 2D band is formed from two elements, namely $2D_1$ and $2D_2$ [45], which are roughly ¼ and ½ of the height of the G peak, respectively. Graphene exhibits a single sharp 2D signal, approximately four times more intense than G band [47]. When more graphene layers are present, the 2D peak is shifted to higher frequencies due to the interactions between the graphene layers.

Many studies showed that Raman spectroscopy can be used as an indicator for single or multi-layer graphene [48]. As one can see the 2D peak evolves as the number of graphene layers increases to about ten layers upon its profile resembles with that of graphite. As the number of graphene layers increases an important reduction of the relatively intensity for the $2D_1$ mode is noticed. Therefore graphene stacks that have more than five layers are more difficult to discriminate from graphite by Raman spectroscopy (**Figure 6**).

It is worth pointing out that this technique for identifying the number of graphene sheets is precisely established only for graphene with AB Bernal stacking [49]. Graphene samples that exhibit AB Bernal stacking features are graphene layers where half of their atoms lie directly over the center of a hexagon in the lower graphene sheet, and half of the atoms lie over an atom. Bernal stacked bilayer graphene exhibit much interest for functional electronic and photonic devices due to the feasibility to continuously tune its band gap with a vertical electrical field [50]. Such type of samples are obtained from highly oriented pyrolytic graphite (HOPG) produced by mechanical exfoliation. Also chemical vapor deposition (CVD) or thermal deposition of SiC can be used to synthetize bilayer graphene but these procedures do not lead to homogeneously AB stacking layers.

Since the graphene flakes have small dimensions it is important to select a Raman instrument with high microscopy performances. Consequently for more accurate results most Raman measurements are performed using an optical microscope which allows a better localization

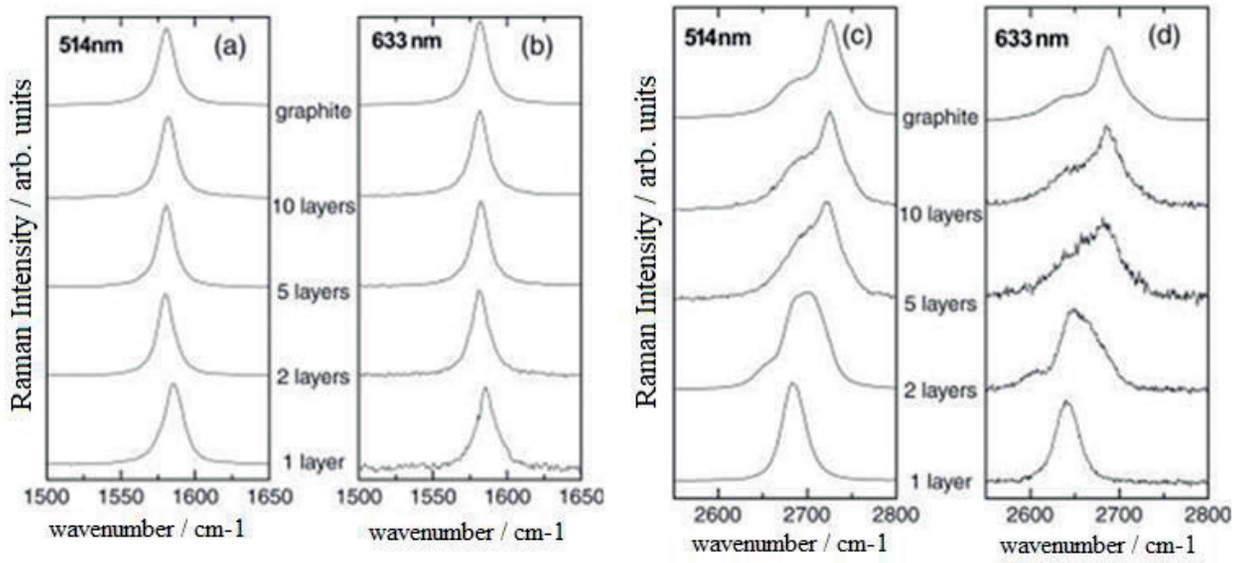

Figure 6. (a) and (b) The evolution of G band by increasing the number of layers, (c) and (d) The evolution of the 2D band by increasing the number of graphene layers using 514 and 633 nm excitation laser (Ferrari A (2007) copyrights).

of the graphene layers. Raman microscopy couples a Raman spectrometer to a standard optical microscope, allowing high magnification visualization of graphene and Raman analysis with a microscopic laser spot.

However, the addition of a microscope to a Raman spectrometer does not provide full 3D spatial resolution. More recently, confocal Raman microscopy (CRM) was used in order to investigate graphene layers [51]. As the name suggests confocal Raman microscopy refers to the ability to spatially filter the analysis volume of the sample, in the XY (lateral) and Z (depth) axes. A confocal microscope practically designs clear images of a sample by removing most of the light from the investigated sample [52]. Apart from allowing better observation of fine details of the sample CRM gives rich information concerning the distribution of individual chemical components, and variation in other effects such as phase, polymorphism, stress/strain, and crystallinity. Based on thousands of Raman spectra acquired from different positions on the sample Raman spectral mapping can be created generating detailed chemical images.

Moreover, the substrate on which the graphene samples are deposited and the Raman equipment performances has a significant role for graphene investigation. Monolayer graphene can be observed on many types of substrates like sapphire, single crystal quartz, glass, metal alloys like NiFe, or polymers like polytetrafluoroethylene (PTFE), but the most popular substrate surface used to discriminate the monolayer graphene is the silicon wafer with a silicon dioxide layer (SiO_2/Si). The Si/SiO_2 substrate usually with 300 nm thickness was reported in many studies as the most appropriate for visual detection of single layer graphene (SLG) [53]. Additionally, it is important to study the interaction between monolayer graphene and the substrate because possible interaction may appear due to defects or surface changes between the two interfaces. In case of monolayer graphene obtained by epitaxial growth from SiC substrates a strong interaction between graphene and SiC substrate appears by strong blue-shifting the G and 2D signals (~11 cm^{-1} and ~34 cm^{-1}, respectively) due to covalent bonding of the two interfaces [54]. On the other hand, the interactions between graphene produced by micro-cleaving and standard SiO_2/Si substrate do not influence the physical structure of graphene because only weak Van der Waals forces could appear [55].

It was found that the Raman spectrum depends not only on the substrate, but also on the wavelength of the excitation laser. Regarding the laser excitation energy for graphene investigation usually the visible lights laser are employed (from 633 to 473 nm). The near infrared (NIR) or ultraviolet (UV) sources are not frequently used. When analyzing graphene layers placed on silicon wafers with silicon dioxide (SiO_2/Si) strong fluorescence signals are observed using a NIR laser (780 or 785 nm). Also, graphene layers are difficult to investigate using a UV excitation laser (from 244 to 364 nm) due to the fact that the obtained Raman spectrum exhibits differences concerning relative intensities of the characteristic graphene signals. Not least the selection of the excitation source is important. In order to avoid sample damaging usually powers between 0.04 to 4 mW are employed. At higher laser power it was observed that the laser may burn the graphene sample leading to graphitization and therefore to spectral variations. Also, if lower laser power is used the ratio between the Raman signal and noise is very poor [56].

Graphene oxide (GO) is another graphene material that can be intense characterized by Raman spectroscopy. By chemical oxidation of graphite in the presence of strong oxidizing agents

and ultrasonic cleavage graphite oxide is obtained, at the end presenting on its surface a significant number of functional groups such as hydroxyl, carboxyl and epoxy [57]. The introduction of oxygenated functionalities not only expands the layer separation, but also makes the material hydrophilic and relatively easy to disperse in aqueous media or other polar solvents [58]. This property enables graphite oxide to exfoliate in hydrophilic medium under sonication and finally to produce single or few layer graphene oxide (GO). Consequently the main difference between graphite oxide and graphene oxide is the number of layers.

In the last decade GO attracted the researchers attention due to its many important properties which can be used to tailor novel applications. Graphene oxide sheets exhibit high design flexibility. GO is decorated with a significant number of carboxyl groups (-COOH) and most of them are located at the GO edges. These carboxyl groups are extremely useful as they can easily react for attachment of various functionalities. Thus, reactions may be established with (a) amines and various organic molecules or polymers which exhibit in their composition amino groups, by forming an amide linkage, (b) alcohols, phenols or epoxy groups to form ester bond, (c) various other organic reactive macromolecules, resulting in the functionalization of GO.

Functionalization of GO can fundamentally change graphene oxide's properties and consequently, graphene oxide's applications. Graphene oxide flakes can be used to remove radioactive ions from water for disposal [59]. Also, graphene oxide can be used to develop sensors that can detect tumorous cells by attaching to GO surfaces molecules that contain antibodies that are further linked to the cancer cells. The cancer cells are then tagged with fluorescent molecules to make the cancer cells stand out in a microscope [60]. Withal graphene oxide is used to obtain anodes for rechargeable lithium-ion batteries. The graphene oxide is thermally treated in order to extract the oxygen form the film and driven to cause pores in the film which are rapidly filled with lithium ions, resulting in quicker charge-discharge process for batteries [61].

With respect to electrical conductivity, graphene oxide behaves as an electrical insulator, because of the disruption of its sp^2 bonding networks. It is important to reduce the graphene oxide so as to restore the honeycomb hexagonal lattice of graphene, in order to recover electrical conductivity. The product of this reduction reaction has been named in different ways, including: reduced graphene oxide (rGO), chemically-reduced graphene oxide (CRGO), and graphene. For the purposes of clarity, we will refer to the product as reduced graphene oxide (rGO). Chemical reduction of graphene oxide is mostly employed in the presence of hydrazine (N_2H_4) where the majority of the oxidized groups of GO are reduced. But the use of anhydrous N_2H_4 demands a dry environment which creates difficulties for the large-scale production. Usually chemical reduction agents are classified as toxic or corrosive. The electrochemical method to reduce graphene oxide in order to produce large rGO films is a greener, safer and more convenient procedure for reducing graphene oxide films. Also the thermal expansion of graphite oxide can be used for exfoliating graphite layers and finally to produce functionalized graphene sheets. Temperatures around 550°C or higher can break the Van der Waals forces that stack the graphene layers together and exfoliation occurs. After the reduction of graphene oxide defect sites within the lattice are produced which provide new routes for chemical functionalization. Chemical modification of the graphene oxide by functionalization with different other molecules or polymers opens new routes for the incorporation of

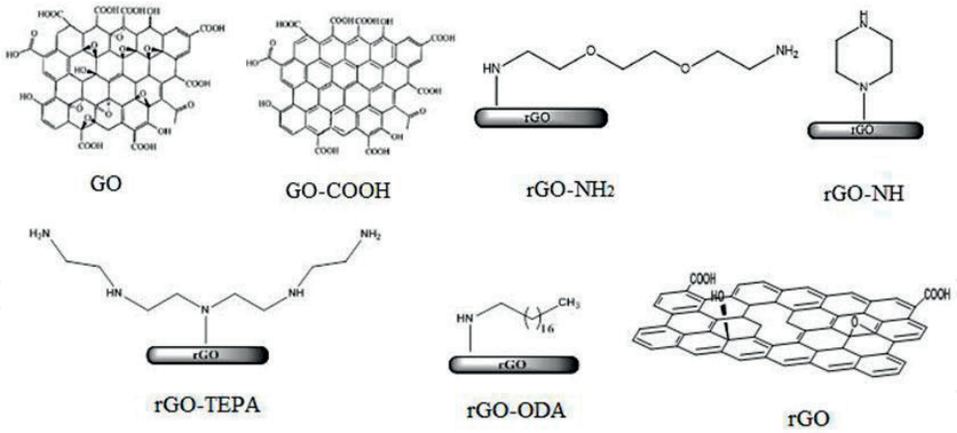

Figure 7. Chemical structures of graphene oxide investigated by Raman spectroscopy.

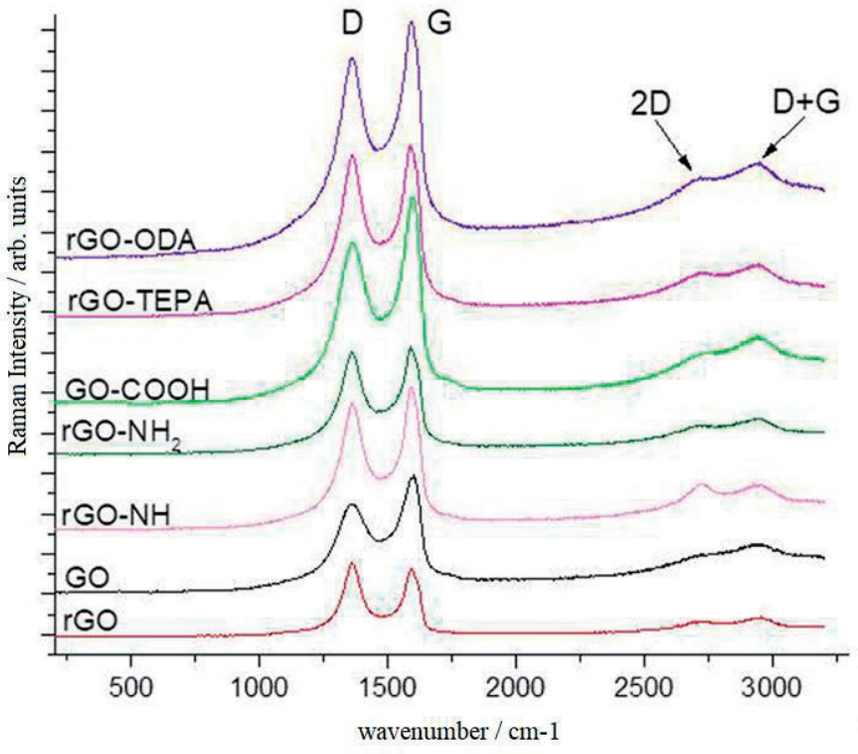

Figure 8. Raman spectra of various graphene oxides.

graphene in other matrices and surfaces to enhance its applicability, that which would otherwise be more difficult using pristine graphene.

Being a derivative of graphene, the graphene oxide structure and functionalized graphene oxide can be also successfully characterized by Raman spectroscopy. For this study different structures of commercial graphene oxide (**Figure 7**) were investigated using a Raman spectrometer equipped with confocal microscope.

In the Raman spectra of the studied graphene oxide structures one can observe that the G band is much broader than in case of graphene and also blue-shifted to ~1590 cm^{-1} (**Figure 8**). The D band from graphene oxide Raman spectra is also modified exhibiting a much higher intensity due to the disorder in the sp^2 structure induced after the oxidation of graphite and also due to the attachment of hydroxyl and epoxide groups on the planar carbon structure. Depending on the functionalization degree of graphene oxide, the Raman spectrum may exhibit sometimes even stronger D band than G band. Regarding the 2D band its intensity is very small compared to the D and G peaks, but may be enhanced by reducing the number of graphene oxide layers. The D+G combination peak is also observed which strongly supports the presence of a higher disorder structure for graphene oxide.

3. Raman investigation of graphene and graphene oxide nanocomposites

Polymeric composites are biphasic materials consisting essentially of a continuous phase, commonly referred to as polymer matrix, and a reinforcing or filler agent, which is the discrete phase. The purpose of this association is to obtain materials with enhanced properties, superior to those of individual components, capable of replacing natural materials (wood, rocks, etc.), aluminum and its alloys, and other metallic materials. Polymeric composites are obtained from a wide range of matrices (epoxy resins, polyester resins, phenol-formaldehyde resins, vinyl polymers, elastomers, polyimides, etc.) with reinforcing materials (boron fibers, glass fibers, or filler materials (wood flour, starch, silica, talc, asbestos, etc.).

Nanocomposites represent a new class of composites, characterized by the coexistence of two distinct phases (an organic one which is the polymer as the continuous phase and an inorganic phase dispersed in the continuous phase, the latter exhibiting nanometric dimensions). The advantages of these structures consist in global properties superior to the individual components such as improved optical clarity, high mechanical resistance, better conductivity, leading to important uses in electronics, optics, constructions, etc. In order to obtain nanocomposites, two important aspects should be considered: firtsly, the nanoparticle must be compatible with the polymer and to show satisfactory interfacial interaction; secondly, the most convenient way to uniformly disperse the nanoparticles in the polymer matrix should be chosen. In most cases polymeric nanomaterials exhibit multifunctionality by combining more than one properties.

When the polymer is unable to intercalate between the graphene layers, a phase separation (two distinct phases) is obtained, the properties of which resemble the microcompounds. In addition to this class, two other types of composites can be prepared: intercalated structures where most of the time a single polymer chain is interposed between layers of graphene, resulting in a multilayered structure in which the polymer-graphene layers alternate and exfoliated structures in which the graphene layers are completely dispersed in the continuous polymer matrix (**Figure 9**).

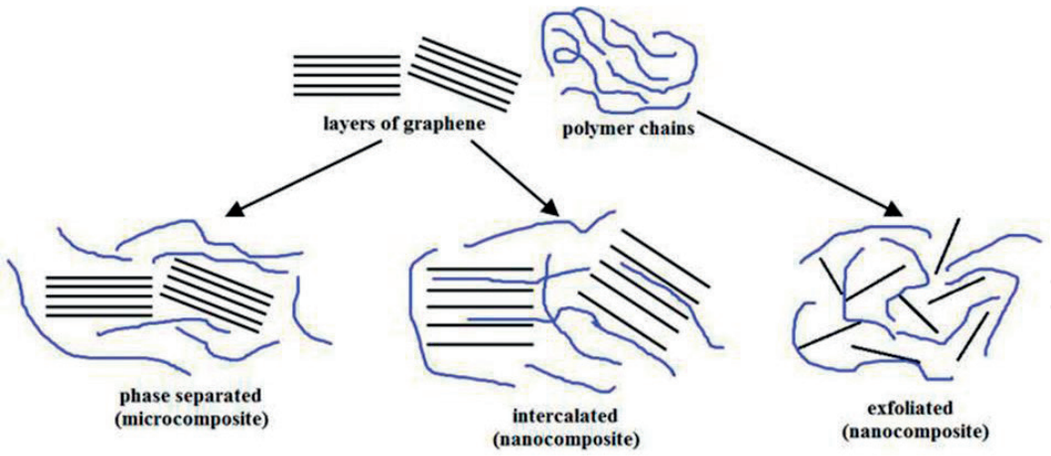

Figure 9. Schematic structure of graphene – based polymer composites.

Graphene nanosheets–polystyrene nanocomposites (GNS-PS) were prepared by in situ emulsion polymerization and reduction of graphene oxide using hydrazine hydrate [62]. The nanocomposites displayed high electrical conductivity, and a considerable increase in glass-transition temperature and good thermal stability of PS are also achieved. Raman spectroscopy was employed as an efficient tool to probe the structural characteristics and properties of graphene and graphene-based materials.

Figure 10 shows a schematic diagram for the formation of the GNS-PS nanocomposites. TEM images revealed polystyrene microspheres with diameters ranging from 90 to 150 nm attached to the graphene surface, particularly along the edges of the stacked nanosheets with a thickness of several nm. This suggests that the compatibility between PS microspheres and GNS is sufficient to obtain nanosized dispersion without an additional surface treatment.

Regarding the Raman spectrum of GNS, two intense features are assigned to the D band at 1331 cm^{-1} and the G band at 1594 cm^{-1}. The G peak was assigned to vibrations of sp^2 carbon atoms. The peak intensity ratio I_D/I_G of GNS nanocomposites was calculated as 1.156. This fact demonstrated the presence of localized sp^3 defects within the sp^2 carbon network, which shows the chemical grafting of polymers to the GNS surface.

The prominent D peak revealed some structural defects are created during the reduction process of the oxidized functional groups, while GNS synthesized through the exfoliation method is considered a more effective route for graphene sheets production. The G band from the GNS Raman spectrum was noticed at 1594 cm^{-1} and upshifted by 5 cm^{-1} in the composites of GNS–PS. By combining the XRD and Raman spectroscopy, Hu and co-workers proved that the substantial structure of the GNS has been maintained after PS microspheres were linked to the edges of the stacked graphene nanoplatelets, which is advantageous for improving the electrical and thermal properties of polymer.

Interest in graphene oxide has increased significantly due to its epoxy, hydroxyl, carbonyl and carboxyl functional groups, allowing its functionalization and the formation of various monomers on its surface. Dispersibility of graphene oxide in water and other solvents makes

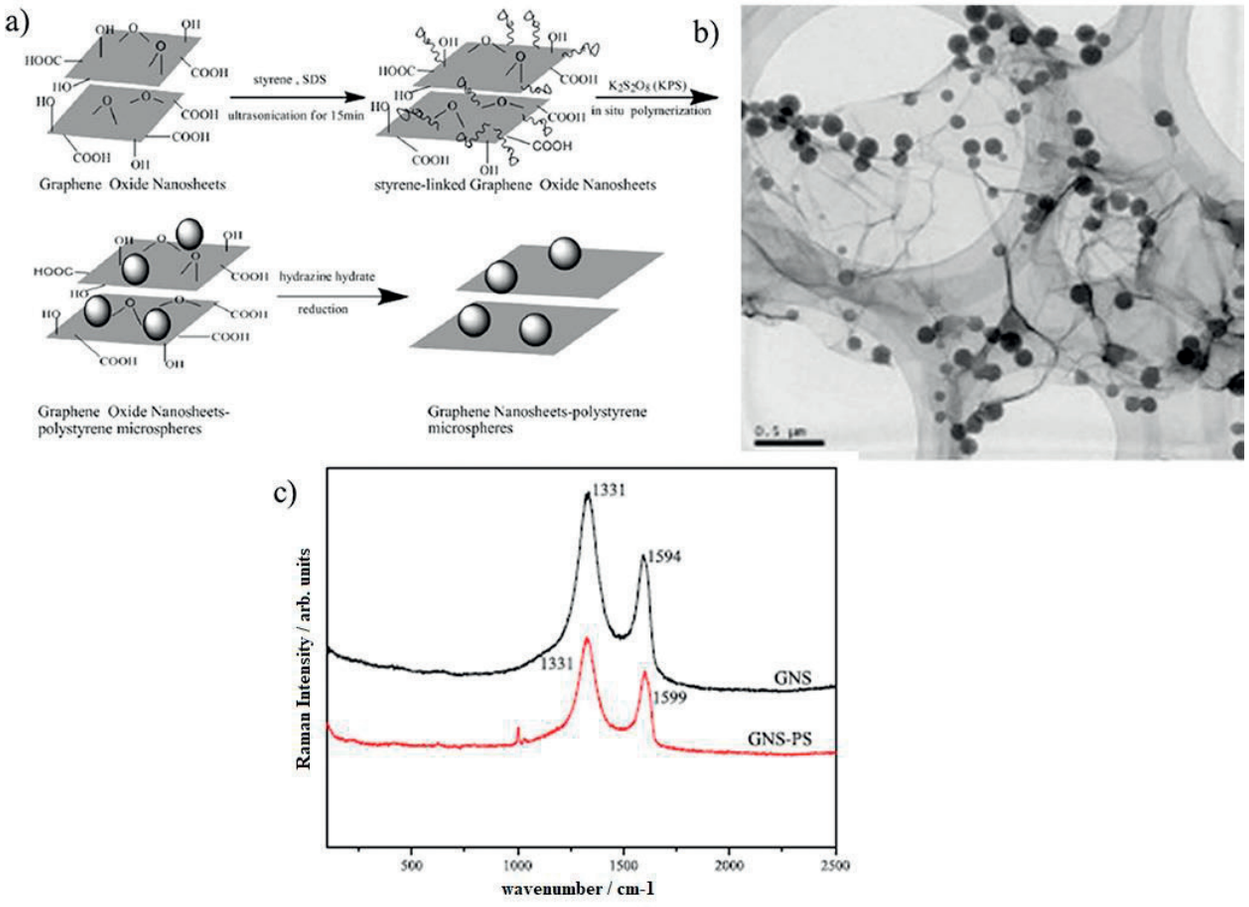

Figure 10. a) Synthesis of GNS-PS nanocomposites; (b) TEM image of CNS-PS nanocomposites; (c) Raman spectra of the pristine GNS and GNS-PS nanocomposites (Hu H et al. (2010) copyrights).

it more attractive compared to graphene for the manufacture of electronic components or in use for nanocomposites synthesis. Polymer reinforced with graphene oxide has been reported in the literature [62].

Recently, graphene oxide with numerous carboxylic groups (GO-COOH) was modified with benzoxazine rings in order to produce exfoliated graphene oxide – polybenzoxazine [63]. The carboxylic groups from GO surface were treated with tyramine (TYR) in order to synthesize a lot of phenolic groups using the activation of the carboxylic groups from GO surface by 1-ethyl-3-(3-dimethylaminopropyl)-carbodiimide/N-Hydroxysuccinimide system (EDC/NHS) and the chlorination method employing $SOCl_2$ respectively. GO-TYR previously obtained further reacted with benzylamine and formaldehyde in order to form the benzoxazine rings. Finally a nano structure with strong covalent bonds between the graphene sheets and the polybenzoxazine chains was achieved (GO-Bz). The study demonstrated that GO-COOH is a good candidate for the preparation of benzoxazine-based nanocomposites due to the abundance of oxidized functional groups on its surface. Raman spectroscopy was successfully employed to demonstrate the efoliation of the graphene sheets through the polybenzoxazine matrix.

In the Raman spectra for the raw material (GO-COOH), GO-TYR and final monomers GO-Bz obtained by both methods, the characteristics of the graphene structure are noticed, namely the intense signals D and G, which proves the presence of the graphene structure in the final compound (**Figure 11**). At the same time, it is worth mentioning the appearance of the 2D band that characterizes the arrangement and the number of graphene plans. Graphene, the two-dimensional form of graphite, consisting of sp^2 hybridized carbon atoms has attracted the attention of researchers in recent years due to its excellent thermal, mechanical, electrical and barrier. All these excellent properties have been shown to the monolayer graphene, the increase of the number of layers leading to the decrease of its properties. For this reason graphene structure has been extensively studied. Raman spectroscopy allows the investigation and determination of the number of layers of the graphene, this information being extracted from the 2D spectrum band. Thus, for products obtained by the EDC/NHS method, the band is wider even in the final benzoxazine product, indicating aggregation in the form of multiple layers of the graphene plans, provided that a part of the benzoxazine monomer did not polymerize and therefore, there was no driving force needed to move the graphene aggregates into independent layers.

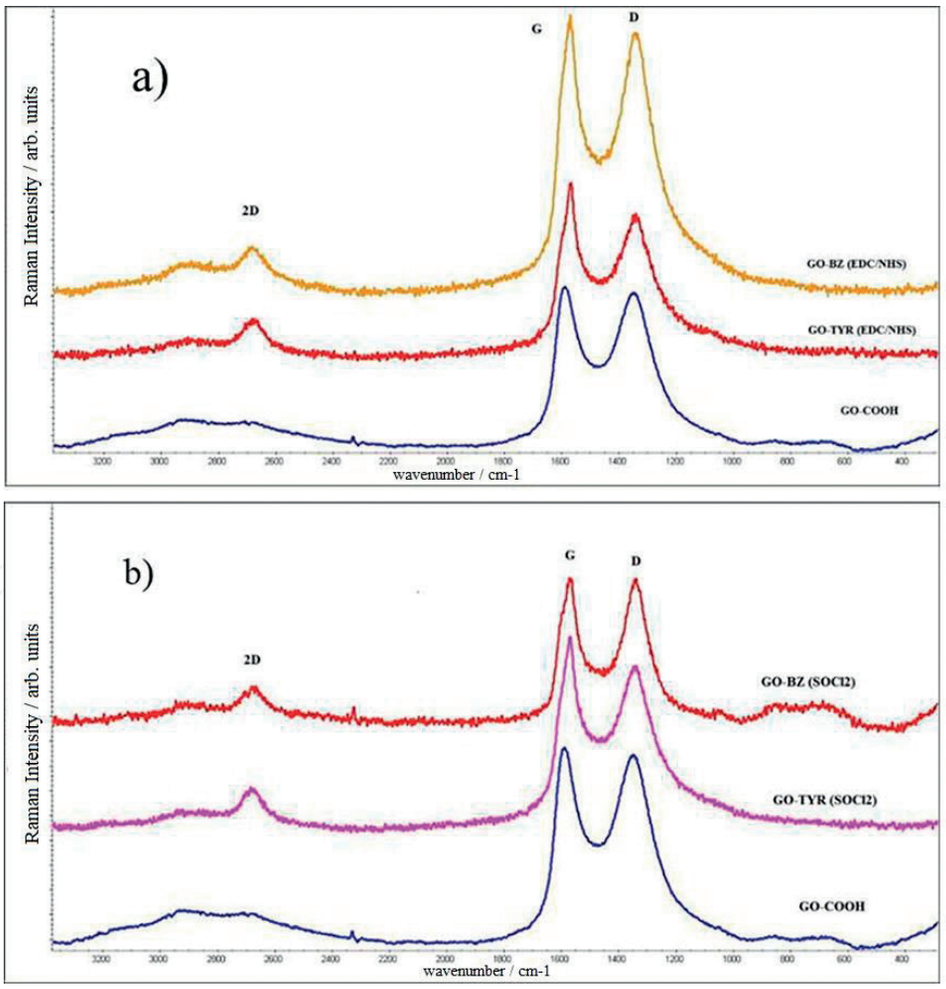

Figure 11. Raman spectra of GO-COOH, GO-TYR, GO-Bz obtained by: a) EDC/NHS activation method; b) chlorination with $SOCl_2$ (Biru I et al. (2016) copyrights).

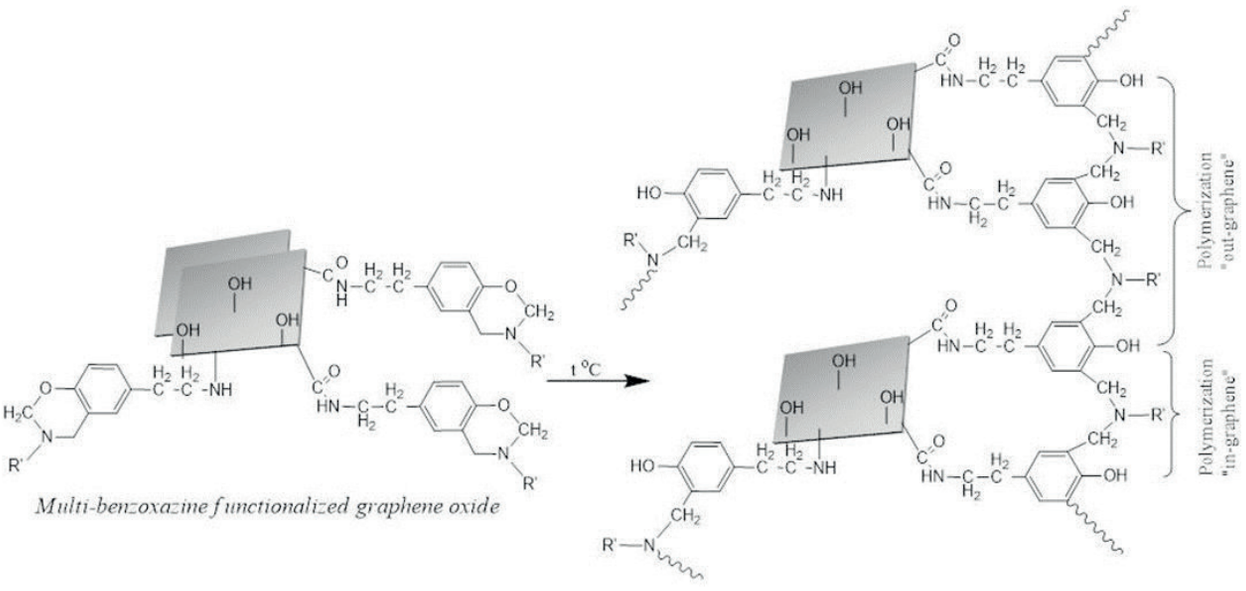

Figure 12. The nanostructure synthesized by polymerization of benzoxazine - functionalized graphene oxide (Biru I et al. (2016) copyrights).

In the case of thionyl chloride products, the 2D band is sharper, which proves that most of the graphene aggregates have disintegrated due to the polymerization of the benzoxazine rings, which has led to the cancellation of the attractions between the graphene plans.

The benzoxazine polymerization may take place either between the rings of the same GO layer ("*in-graphene*" polymerization) or between the rings of two neighbors of GO layers ("*outgraphene*" polymerization). The final balance between these two types of structure will give the ratio between intercalated and exfoliated structures. Consequently the "*in-graphene*" polymerization will lead to more exfoliated structures of GO-Bz (**Figure 12**).

4. Conclusions and outlook

Raman spectroscopy is a powerful instrument for investigating carbon nanomaterials. As a highly sensitive technique Raman spectroscopy is recommended for detection of small changes in structural morphology of various carbon nanomaterials playing an important role as a direct or complementary tool in any laboratory working with carbon allotropes. Raman spectrum shows specific signals for each carbon allotrope when the monochromatic radiation interacts with the sample. Diamond and graphite exhibit significant differences in the Raman spectrum even if both are entirely made of C-C bonds. The Raman spectrum of pure diamond exhibits an extremely sharp signal at ~1332 cm^{-1} which arises from the stretching of the C-C bond. Instead, in the Raman spectrum of graphite two distinguishable peaks are revealed at ~1350 cm^{-1} (D band) and ~1580 cm^{-1} (G band) revealing that the graphite is not as uniform in structure as diamond.

Also more complex structures can be investigated by Raman spectroscopy. The Raman spectrum of C60 fullerene exhibits strong signals at 1467 cm^{-1} and 1567 cm^{-1} revealing that C60 is composed

of sp^2 bonded carbon. The sharpness of the signal shows that C60 exhibits a uniform structure. On the contrary, the Raman spectrum of C70 exhibits numerous other peaks. In case of C70 sample, the main peaks are located at 1564 $cm^{-1}$and 1228 cm^{-1} due to a reduction in molecular symmetry which results in more Raman bands.

With this technique it is easily possible to distinguish graphite from diamond, SWCNTs from MWCNTs or graphene form bulk graphite. The stretching of the C-C bond in graphitic materials gives rise to the G-band Raman feature which is common to all sp^2 carbon systems. The G-band of SWCNTs splits in two band components because of large diameter nanotubes and it can be used to distinguish metallic and semiconducting nanotubes. In case of CNTs the D band is significantly increased compared to graphite indicating that some disorder of the graphene sheets is induced. The radial breathing mode (RBM) is particularly important for the determination of the diameter of CNT, its frequency being related to the aggregation state of SWCNTs. The RBM band is unique to SWNCTs and corresponds to the expansion and contraction of the nanotubes.

Raman spectroscopy could be even used to discriminate single layer graphene from multilayer graphene and to determine number of graphene sheets. In case of pure graphene a sharper 2D band situated at ~2700 cm^{-1} is observed. The 2D band originates from a two-phonon double resonance process and it is interrelated to the band structure of graphene layers. The 2D peak evolves as the number of graphene layers increases to about ten layers upon its profile resembles with that of graphite. Moreover, as a non-destructive characterization technique Raman spectroscopy is frequently used to investigate graphene nanocomposites in order to prove successfully graphene functionalization.

Acknowledgements

This research study was supported by a grant of Ministery of Research and Innovation, CNCS - UEFISCDI, project number PN-III-P4-ID-PCE-2016-0818, within PNCDI III. The authors gratefully acknowledge financial support of the GEX project no. 75/25.09.2017, CH 38-17-05. All data presented were recorded using the Renishaw confocal spectrometer with 473 nm laser excitation wavelength and 1.25 laser power. For this study graphene oxides with different types of functionalities were used as received from NanoInnova Technologies. Graphite, SWCNTs and MWCNTs were purchased from Aldrich.

Author details

Elena Iuliana Bîru[1] and Horia Iovu[1,2]*

*Address all correspondence to: horia.iovu@upb.ro

1 Advanced Polymer Materials Group, University Politehnica of Bucharest, Romania

2 Academy of Romanian Scientists, Romania

References

[1] Cantarero A. Raman scattering applied to materials science. Procedia Material Science. 2015;**9**:113-122. DOI: 10.1016/j.mspro.2015.04.014

[2] Toniazzo V, Mustin C, Benoit R, Humbert B, Berthelin J. Superficial compounds produced by Fe(III) mineral oxidation as essential reactants for bio-oxidation of pyrite by Thiobacillus ferrooxidans. Process Metallurgy. 1999;**9**:177-186. DOI: 10.1016/S1572-4409(99)80017-0

[3] Dégardin K, Desponds A, Roggo Y. Protein-based medicines analysis by Raman spectroscopy for the detection of counterfeits. Forensic Science International. 2017;**278**:313-325. DOI: 10.1016/j.forsciint.2017.07.012

[4] Zhang Z, Wang H, Zhang Y, Mu X, Huang B, Du J, Zhou J, Pan X, Xie E. Carbon nanotube/hematite core/shell nanowires on carbon cloth for supercapacitor anode with ultrahigh specific capacitance and superb cycling stability. Chemical Engineering Journal. 2017;**325**:221-228. DOI: 10.1016/j.cej.2017.05.045

[5] Mousaviac H, Jalilvanda S, Kurdestany JM, Grabowskic M. Electron doping effects on the electrical conductivity of zigzag carbon nanotubes and corresponding unzipped armchair graphene nanoribbons. Physica E: Low-dimensional Systems and Nanostructures. 2017;**94**:87-91. DOI: 10.1016/j.physe.2017.07.026

[6] Bora C, Bharali P, Baglari S, Dolui SK, Konwar BK. Strong and conductive reduced graphene oxide/polyester resin composite films with improved mechanical strength, thermal stability and its antibacterial activity. Composites Science and Technology. 2013; **87**:1-7. DOI: 10.1016/j.compscitech.2013.07.025

[7] Han C, Gu A, Liang G, Yuan L. Carbon nanotubes/cyanate ester composites with low percolation threshold, high dielectric constant and outstanding thermal property. Composites Part A Applied Science and Manufacturing. 2017;**41**:1321-1328. DOI: 10.1016/j.compositesa.2010.05.016

[8] Zhang R, Zhang Y, Zhang Q, Xie H, Qian W, Wei F. Growth of half-meter long carbon nanotubes based on Schulz-Flory distribution. ACS Nano. 2013;**7**:6156-6161. DOI: 10.1021/nn401995z

[9] Chang C, Hsu I, Aykol M, Hung WH, Chen CC, Cronin SB. A new lower limit for the ultimate breaking strain of carbon nanotubes. ACS Nano. 2010;**4**:5095-5100. DOI: 10.1021/nn100946q

[10] Geim AK, Novoselov KS. The rise of graphene. Nature Materials. 2007;**6**:183-191. DOI: 10.1038/nmat1849

[11] Neto AC, Geim A. Graphene: Graphene's properties. New Scientist. 2012;**214**:4-5. DOI: 10.1016/S0262-4079(12)61116-6

[12] Tong Y, Bohm S, Song M. The capability of graphene on improving the electrical conductivity and anti-corrosion properties of polyurethane coatings. Applied Surface Science. 2017;**424**:72-81. DOI: 10.1016/j.apsusc.2017.02.081

[13] Kim H, Ahn J-H. Graphene for flexible and wearable device applications. Carbon. 2017;**120**:244-257. DOI: 10.1016/j.carbon.2017.05.041

[14] Lukowiak A, Kedziora A, Strek W. Antimicrobial graphene family materials: Progress, advances, hopes and fears. Advances in Colloid and Interface Science. 2016;**263**:101-112. DOI: 10.1016/j.cis.2016.08.002

[15] PapageorgiouIan DG, Kinloch A, Young RJ. Mechanical properties of graphene and graphene-based nanocomposites. Progress in Materials Science. 2017;**90**:75-127. DOI: 10.1016/j.pmatsci.2017.07.004

[16] Dobrota AS, Pašti IA, Mentusa SV, Johansson B, Skorodumova NV. Functionalized graphene for sodium battery applications: The DFT insights. Electrochimica Acta. 2017; **250**:185-195. DOI: 10.1016/j.electacta.2017.07.186

[17] Yao K, Dai B, Zhu J, Ralchenko V, Shu G, Zhao J, Wang P, Liu B, Gao G, Sun M, Liu K, Lv Z, Yang L, Han J. Diamond micropowder synthesis via graphite etching in a microwave hydrogen plasma. Powder Technology. 2017;**322**:124-130. DOI: 10.1016/j.powtec. 2017.09.021

[18] Amendolaa V, Matteib G, Cusanc C, Pratoc M, Meneghetti M. Fullerene non-linear excited state absorption induced by gold nanoparticles light harvesting. Synthetic Metals. 2005;**155**:283-286. DOI: 10.1016/j.synthmet.2005.01.032

[19] Papavasileiou KD, Avramopoulos A, Leonis G, Papadopoulos MG. Computational investigation of fullerene-DNA interactions: Implications of fullerene's size and functionalization on DNA structure and binding energetics. Journal of Molecular Graphics and Modelling. 2017;**74**:177-192. DOI: 10.1016/j.jmgm.2017.02.015

[20] Tran CM, Sakai H, Kawashima Y, Ohkubo K, Fukuzumi S, Murata H. Multi-level non-volatile organic transistor-based memory using lithium-ion-encapsulated fullerene as a charge trapping layer. Organic Electronics. 2017;**45**:234-239. DOI: 10.1016/j.orgel. 2017.03.018

[21] Zhang X, Ai X, Zhang R, Ma Q, Wang Z, Qin G, Wang J, Wang S, Suzuki K, Miyazaki T, Mizukami S. Spin conserved electron transport behaviors in fullerenes (C60 and C70) spin valves. Carbon. 2016;**106**:202-207. DOI: 10.1016/j.carbon.2016.05.011

[22] Xia K, Zhan H, Gu Y. Graphene and carbon nanotube hybrid structure: A review. Procedia IUTAM. 2017;**21**:94-101. DOI: 10.1016/j.piutam.2017.03.042

[23] Hedman D, Larsson JA. Length dependent stability of single-walled carbon nanotubes and how it affects their growth. Carbon. 2017;**116**:443-447. DOI: 10.1016/j.carbon. 2017.02.007

[24] Suna L, Wanga X, Wanga Y, Zhang Q. Roles of carbon nanotubes in novel energy storage devices. Carbon. 2017;**122**:462-474. DOI: 10.1016/j.carbon.2017.07.006

[25] Arora N, Sharma NN. Arc discharge synthesis of carbon nanotubes: Comprehensive review. Diamond and Related Materials. 2017;**50**:135-150. DOI: 10.1016/j.diamond. 2014.10.001

[26] Santiago EV, López SH, Camacho López MA, Contreras DR, Mancilla RF, Flores-Gallardo SG, Hernández-Escobar CA, Zaragoza-Contreras EA. Optical properties of carbon nanostructures produced by laser irradiation on chemically modified multi-walled carbon nanotubes. Optics & Laser Technology. 2016;**84**:53-58. DOI: 10.1016/j.optlastec.2016.05.002

[27] Lopez D, Abe IY, Pereyra I. Temperature effect on the synthesis of carbon nanotubes and core–shell Ni nanoparticle by thermal CVD. Diamond and Related Materials. 2015;**52**:59-65. DOI: 10.1016/j.diamond.2014.12.006

[28] Soares OSGP, Rocha RP, Gonçalves AG, Figueiredo JL, Órfão JJM, Pereira MFR. Easy method to prepare N-doped carbon nanotubes by ball milling. Carbon. 2015;**91**:114-121. DOI: 10.1016/j.carbon.2015.04.050

[29] Anoshkin IV, Nefedova II, Lioubtchenko DV, Nefedov IS, Räisänen AV. Single walled carbon nanotube quantification method employing the Raman signal intensity. Carbon. 2017;**116**:547-552. DOI: 10.1016/j.carbon.2017.02.019

[30] Varga M, Izak T, Vretenar V, Kozak H, Holovsky J, Artemenko A, Hulman M, Skakalova V, Lee DS, Kromka A. Diamond/carbon nanotube composites: Raman, FTIR and XPS spectroscopic studies. Carbon. 2017;**111**:54-61. DOI: 10.1016/j.carbon.2016.09.064

[31] Powell C, Beall GW. Graphene oxide and graphene from low grade coal: Synthesis, characterization and applications. Current Opinion in Colloid & Interface Science. 2015;**20**:362-366. DOI: 10.1016/j.cocis.2015.11.003

[32] Guo L, Yin X, Wu W, Meng H. Preparation of graphene via liquid-phase exfoliation with high gravity technology from edge-oxidized graphite. Colloids and Surfaces A: Physicochemical and Engineering Aspects. 2017;**531**:25-31. DOI: 10.1016/j.colsurfa.2017.07.074

[33] Konishi K, Cui Z, Hiraki T, Yoh K. Spin-injection into epitaxial graphene on silicon carbide. Journal of Crystal Growth. 2013;**378**:385-387. DOI: 10.1016/j.jcrysgro.2012.12.168

[34] Liu Z, Lin L, Ren H, Sun X. CVD synthesis of Graphene. A volume in Micro and Nano Technologies (Elsevier). 2017:19-56. DOI: 10.1016/B978-0-32-346240-2.00002-9

[35] Toh SY, Loh KS, Kamarudin SK, Daud WRW. Graphene production via electrochemical reduction of graphene oxide: Synthesis and characterisation. Chemical Engineering Journal. 2014;**251**:422-434. DOI: 10.1016/j.cej.2014.04.004

[36] Zhong Y, Zhen Z, Zhu H. Graphene: Fundamental research and potential applications. FlatChem. 2017;**4**:20-32. DOI: 10.1016/j.flatc.2017.06.008

[37] Vasić B, Matković A, Ralević U, Belić M, Gajić R. Nanoscale wear of graphene and wear protection by graphene. Carbon. 2017;**120**:137-144. DOI: 10.1016/j.carbon.2017.05.036

[38] Piattia E, Galassoa S, Tortelloa M, Naira JR, Gerbaldia C, Brunab M, Borinib S, Dagheroa D, Gonnelli RS. Carrier mobility and scattering lifetime in electric double-layer gated few-layer graphene. Applied Surface Science. 2017;**395**:37-41. DOI: 10.1016/j.apsusc.2016.06.192

[39] Yang W, Ni M, Ren X, YafenTian NL, Sub Y, Zhang X. Graphene in Supercapacitor applications. Current Opinion in Colloid & Interface Science. 2015;**20**:416-428. DOI: 10.1016/j.cocis.2015.10.009

[40] Han T, Kim H, Kwon SJ, Lee TW. Graphene-based flexible electronic devices. Materials Science & Engineering R: Reports. 2017;**118**:1-43. DOI: 10.1016/j.mser.2017.05.001

[41] Cao L, Zhang F, Wang Q, Fabrication XW. Of chitosan/graphene oxide polymer nanofiber and its biocompatibility for cartilage tissue engineering. Materials Science and Engineering: C. 2017;**79**:697-701. DOI: 10.1016/j.msec.2017.05.056

[42] Naskar A, Khan H, Bera S, Jana S. Soft chemical synthesis, characterization and interaction of ZnO graphene nanocomposite with bovine serum albumin protein. Journal of Molecular Liquids. 2017;**237**:113-119. DOI: 10.1016/j.molliq.2017.04.074

[43] Justino CIL, Gomes AR, Freitas AC, Duarte AC, Rocha-Santos TAP. Graphene based sensors and biosensors. TrAC Trends in Analytical Chemistry. 2017;**91**:53-66. DOI: 10.1016/j.trac.2017.04.003

[44] Mishra S, Ashaduzzamana M, Mishra P, Swart HC, Turner APF, Tiwari A. Stimuli-enabled zipper-like graphene interface for auto-switchable bioelectronics. Biosensors and Bioelectronics. 2017;**89**:305-311. DOI: 10.1016/j.bios.2016.03.052

[45] Gokhale AA, Lu J, Lee I. Immobilization of cellulase on magnetoresponsive graphene nano-supports. Journal of Molecular Catalysis B: Enzymatic. 2013;**90**:76-86. DOI: 10.1016/j.molcatb.2013.01.025

[46] Ghany NA, Elsherif SA, Handal HT. Revolution of Graphene for different applications: State-of-the-art. Surfaces and Interfaces. 2017;**9**:93-106. DOI: 10.1016/j.surfin.2017.08.004

[47] Ferrari AC. Raman spectroscopy of graphene and graphite: Disorder, electron–phonon coupling, doping and nonadiabatic effects. Solid State Communications. 2007;**143**:47-57. DOI: 10.1016/j.ssc.2007.03.052

[48] Ferrari AC, Meyer JC, Scardaci V, Casiraghi C, Lazzeri M, Mauri F, Piscanec S, Jiang D, Novoselov KS, Roth S, Geim AK. Raman Spectrum of Graphene and Graphene layers. Physical Review Letters. 2006;**97**:187401. DOI: 10.1103/PhysRevLett.97.187401

[49] Malard LM, Pimenta MA, Dresselhaus G, Dresselhaus MS. Raman spectroscopy in graphene. Physics Reports. 2009;**473**:51-87. DOI: 10.1016/j.physrep.2009.02.003

[50] Liu L, Zhou H, Cheng R, Yu WJ, Liu Y, Chen Y, Shaw J, Zhong X, Huang Y, Duan X. High yield chemical vapor deposition growth of high quality large-area AB stacked bilayer graphene. ACS Nano. 2012;**6**:8241-8249. DOI: 10.1021/nn302918x

[51] Peng H, Sun M, Zhang D, et al. Raman spectroscopy of graphene irradiated with highly charged ions. Surface and Coatings Technology. 2016;**306**:171-175. DOI: 10.1016/j.surfcoat.2016.05.064

[52] Semwogerere D, Weeks ER. Confocal Microscpy. Encyclopedia of Biomaterials and Biomedical Engineering. London: Taylor & Francis; 2005. pp. 1-10. DOI: 10.1081/E-EBBE-120024153

[53] Gui Y, Sun H. Effects of substrates on Raman spectroscopy in chemical vapor deposition grown graphene transferred with poly (methyl methacrylate). Solid State Communications. 2017;**264**:31-34. DOI: 10.1016/j.ssc.2017.04.010

[54] Ni Z, Wang Y, Yu T, Shen Z. Raman spectroscopy and imaging of graphene. Nano Research. 2008;**1**:273-291. DOI: 10.1007/s12274-008-8036-1

[55] Calizo I, Ghosh S, Bao W, Miao F, Lau CN, Balandin AA. Raman nanometrology of graphene: Temperature and substrate effects. Solid State Communications. 2009;**149**:1132-1135. DOI: 10.1016/j.ssc.2009.01.036

[56] Ferrari AC, Robertson J. Raman spectroscopy in carbons: From nanotubes to diamond. Philosophical Transactions of the Royal Society A. 2008;**362**:2267-2565

[57] Yuan R, Yuan J, Wu Y, Chen L, Zhou H. Jianmin Chen. Efficient synthesis of graphene oxide and the mechanisms of oxidation and exfoliation. Applied Surface Science. 2017; **416**:868-877. DOI: 10.1016/j.apsusc.2017.04.181

[58] Liu Y, Zhang Y, Duan L, Zhang W, Su M, Sun Z, He P. Polystyrene/graphene oxide nanocomposites synthesized via Pickering polymerization. Progress in Organic Coatings. 2016;**99**:23-31. DOI: 10.1016/j.porgcoat.2016.04.034

[59] Zong P, Cao D, Cheng Y, Zhang H, Shaoc D, Wangad S, Hee C, Zhao Y. Functionally reduced graphene oxide supported iron oxides composites as an adsorbent for the immobilization of uranium ions from aqueous. Journal of Molecular Liquids. 2017;**240**:578-588. DOI: 10.1016/j.molliq.2017.05.101

[60] Bahreyni A, Yazdian-Robati R, Hashemitabar S, Ramezani M, Ramezani P, Abnous K, Taghdis SM. A new chemotherapy agent-free theranostic system composed of graphene oxide nano-complex and aptamers for treatment of cancer cells. International Journal of Pharmaceutics. 2017;**526**:391-399. DOI: 10.1016/j.ijpharm.2017.05.014

[61] Yan L, Yu J, Luo H. Ultrafine TiO_2 nanoparticles on reduced graphene oxide as anode materials for lithium ion batteries. Applied Materials Today. 2017;**8**:31-34. DOI: 10.1016/j.apmt.2017.02.001

[62] Hu H, Wang X, Wanga J, Wana L, Liu F, Zhen H, Chen R, Xu C. Preparation and properties of graphene nanosheets–polystyrene nanocomposites via in situ emulsion polymerization. Chemical Physics Letters. 2010;**484**:247-253. DOI: 10.1016/j.cplett.2009.11.024

[63] Biru I, Damian CM, Gârea SA, Iovu H. Benzoxazine - functionalized graphene oxide for synthesis of new nanocomposites. European Polymer Journal. 2016;**83**:244-255. DOI: 10.1016/j.eurpolymj.2016.08.024

IntechOpen